Available online at www.sciencedirect.com
ScienceDirect
Ceramics International 37 (2011) 921–926
CERAMICS INTERNATIONAL
www.elsevier.com/locate/ceramint

High temperature bending creep behavior of a multi-cation doped α/β-SiAlON composite

Alper Uludağ *, Dilek Turan

Anadolu University, School of Civil Aviation, Iki Eylul Campus, 26470 Eskisehir, Turkey

Received 2 August 2010; received in revised form 20 August 2010; accepted 29 October 2010
Available online 8 January 2011

Abstract

SiAlON ceramics with high hardness and high toughness can be made through designing α/β-SiAlON composites. An important advantage of α-SiAlON phase is that the amount of intergranular phase is reduced by the transient liquid phase being absorbed into the matrix of α-SiAlON phase during sintering. But, the thermal stability of the α-SiAlON phase is an important concern for α/β-SiAlON composites especially at high temperatures. The use of different types of single or multiple cations during fabrication directly affects resultant microstructures and mechanical behavior of α/β-SiAlON composites. In this study, the creep behavior of a multi-cation (Y, Sm and Ca) doped α/β-SiAlON composite, in which aluminum-containing nitrogen melilite solid solution phase was designed as intergranular phase, was investigated by four-point bending creep tests under stresses from 50 to 150 MPa and at temperatures from 1300 °C to 1400 °C in air. The stress exponent was determined to be 1.6 ± 0.13 at 1400 °C and the creep activation energy was calculated to be 692 ± 37 kJ/mol^{-1}. Grain boundary sliding coupled with diffusion was identified as the rate-controlling creep mechanism for the α/β-SiAlON composite.

Keywords: C. Creep; α/β-SiAlON; Aluminum-containing nitrogen melilite

1. Introduction

Silicon nitride (Si_3N_4) is one of the major structural ceramics that has been developed following many years of intensive research. It possesses high flexural strength, high fracture resistance, good creep resistance, high hardness and excellent wear resistance [1]. These excellent properties offer great potential in structural applications [2]. On the other hand, other important structural material SiAlONs generally consist of two crystalline phases: α-SiAlON and β-SiAlON which are isostructural with α-Si_3N_4 and β-Si_3N_4, respectively [3]. An important advantage of α-SiAlONs is that the amount of intergranular phase is reduced by the transient liquid phase being absorbed into the matrix of α-SiAlON phase during sintering. As α-SiAlON and β-SiAlON phases are completely compatible, SiAlON ceramics with both higher hardness and higher toughness can be achieved through designing of α/β-SiAlON composites [4]. Meanwhile, the combination of SiAlON phases has a great influence on mechanical properties of SiAlON ceramics. Due to the different microstructure and composition, α and β-SiAlON have distinct contribution to creep resistance [5,6]. Klemm et al. pointed out that creep resistance was enhanced with the increase of α-SiAlON content in the study of four point bending creep of α/β-SiAlON composite using YAG as intergranular phase. They attributed the improved creep resistance to the thinner grain boundaries between α-SiAlON grains and a strong creep resistance of skeleton [5].

The two common methods for improving high-temperature properties of Si_3N_4 based ceramics are (i) increasing the softening point of the amorphous phases above the temperature range to which the ceramic will be exposed and (ii) crystallization of the amorphous phases, so as to eliminate the softening point entirely [2,7]. Therefore, one of the main aspects in designing SiAlONs with improved high temperature properties would be to use additives that would provide a good liquid phase sintering behavior and at the same time would crystallize well to refractory phases after sintering. In this study, Y–Sm–Ca multi cation system was chosen to produce hard and

* Corresponding author.
E-mail addresses: alperuludag@anadolu.edu.tr (A. Uludağ), dtetik@anadolu.edu.tr (D. Turan).

0272-8842/$36.00
doi:10.1016/j.ceramint.2010.11.012

tough α/β-SiAlON composite for high temperature applications [8]. To prevent the side effect of intergranular phase, refractory aluminum-containing nitrogen melilite ($Ln_2Si_{3-x}Al_xO_{3+x}N_{4-x}$) phase crystallization was aimed. There is little information in the literature concerning creep of SiAlON ceramics with multi cation sintering additives. Therefore, the objective of the present work is to investigate the creep behavior of new multi-cation doped α/β-SiAlON ceramics.

2. Experimental procedure

The overall composition of the prepared starting powder mixtures were corresponding to duplex α/β SiAlON ceramic with 25α/75β ratio. Starting powder mixtures were prepared using α-Si_3N_4 (UBE-E10) with AlN (HC Starck-Berlin, Grade C), Al_2O_3 (Alcoa, Grade A16SG) together with mixtures of Y_2O_3 (H.C. Starck Berlin), Sm_2O_3 (Stanford Materials Corp.) and CaO (Reidel-de Haen) as densifying additives. The powder mixtures with binding materials were uniaxially pressed under 50 MPa as bar shape and subsequently cold isostatically pressed at 300 MPa to improve green density. After de-binding process, the bar specimens were gas pressure sintered under N_2 atmosphere at different times and temperatures. The densities of the sintered bodies were measured by using the water-displacement method.

The creep test specimens were first machined by surface grinding in a direction parallel to the length of the fully densified specimens with 80–350 grit diamond resinoid bonded wheels until having dimensions of 3 mm in height, 4 mm in width, and 50 mm in length. They were then mechanically polished and the edges of all specimens were chamfered. Creep tests were conducted on four-point bending fixture made of SiC with inner and outer span of 20 mm and 40 mm, respectively by using of an Instron 5581 testing machine. The flexure creep strain of the creep specimen was measured by using transducer rod connected to a linear-variable differential transducer (LVDT) and recorded by a computer.

The phase compositions and substitution levels as-sintered and crept samples were determined by using an X-ray powder diffractometer (XRD, Rigaku Rint 2000). The α-SiAlON: β-SiAlON ratio was calculated using the relative intensities from X-ray analyses of the peaks of α (1 0 2, 2 1 0) and β (1 0 2, 2 1 0) [9].

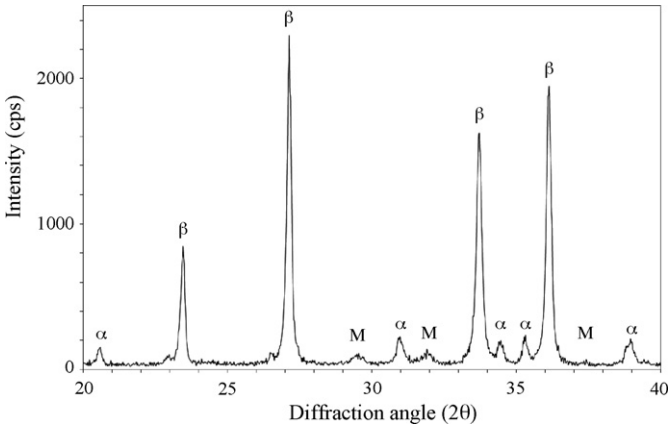

Fig. 1. X-ray diffraction pattern of as-sintered α/β-SiAlON ceramic (β: beta SiAlON phase, α: alpha SiAlON phase, M: melilite phase ($Ln_2Si_{3-x}Al_xO_{3+x}N_{4-x}$)).

In order to find out the effect of the creep on the microstructure of α/β-SiAlON ceramics, the microstructures of as-sintered and crept samples were investigated by using scanning electron microscope (SEM-ZEISS SUPRA 50 VP) attached with an energy dispersive X-ray spectrometer (EDX-Oxford Inca) and transmission electron microscope (TEM-JEOL 2100F) attached with a scanning transmission electron microscope (STEM) high angle annular dark field detector.

3. Results and discussion

3.1. Phase composition and microstructural characterization of noncrept materials

XRD pattern from the gas pressure sintered α/β-SiAlON ceramic in Fig. 1 showed large peaks from α-SiAlON and β-SiAlON, as well as small peaks from other crystalline phase(s). The α/β phase ratio was found to be around 25α/75β-SiAlON as designed for this study. An analysis of the small peaks in the pattern indicated the formation of crystalline aluminum-containing nitrogen melilite phase ($Ln_2Si_{3-x}Al_xO_{3+x}N_{4-x}$) (Fig. 1).

The back-scattered SEM image of as-sintered α/β-SiAlON composite is given in Fig. 2 showing that the microstructure consists of α and β-SiAlON grains, and triple-junction pockets

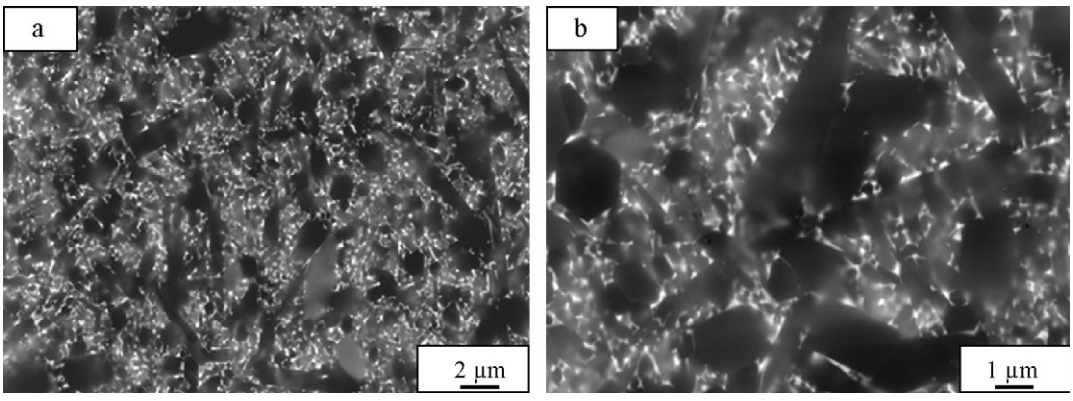

Fig. 2. Back-scattered SEM images of as sintered α/β-SiAlON composite (a) 10,000× and (b) 20,000×.

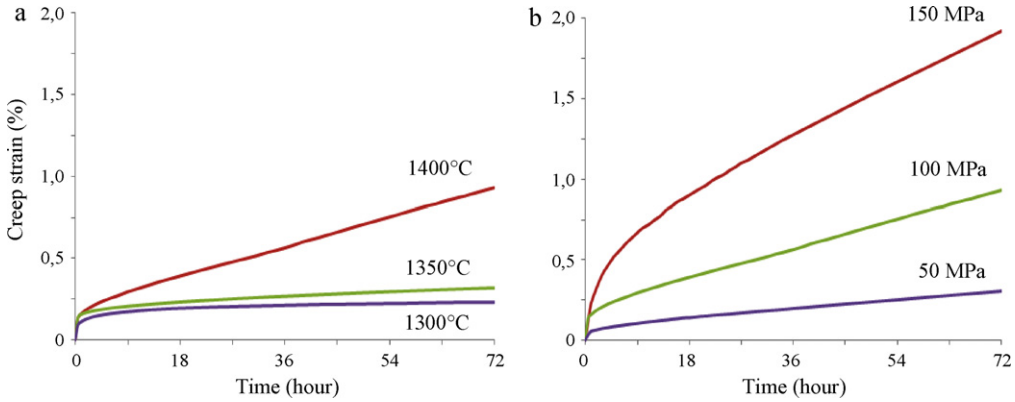

Fig. 3. Creep behavior of as-sintered α/β-SiAlON composite as a function of temperature (a) and stress (b).

filled with remains of the liquid formed during sintering. The triple-junction regions were homogeneously distributed throughout the samples. Detailed X-ray diffraction investigations showed that some of the triple junction phases in the Y–Sm–Ca multi cation doped ceramic were crystalline [8].

3.2. Creep behavior and mechanisms

Flexure creep tests were conducted with as-sintered fully densified specimens in order to find out the creep behavior of SiAlON ceramics, in air at temperatures ranging between 1300 and 1400 °C and under stress levels ranging from 50 to 150 MPa. All tests were finished after 72 h, without evidence of macroscopic failure. The flexure creep strain–time curves obtained in this study is given in Fig. 3. All the measured flexure creep strain-time curves show primary and secondary creep, but no tertiary creep. Si_3N_4 based ceramics typically show only primary and secondary creep [10–16]. Stress rupture occurs in the secondary creep region because of the relatively brittle nature of Si_3N_4 based ceramics.

The time for primary creep is determined to be between 5 and 20 h depending on the testing conditions. The primary creep was followed by a steady state, nearly constant, creep rate. In secondary creep the strain rates were relatively low, but the specimens especially at 1400 °C deformed most in this stage; about 60–70% of the total deformation occurred. The steady strain rates obtained from all creep tests conditions are given in Table 1. When the steady strain rates (Table 1) is examined, it can be seen that the steady strain rates normally increase while test temperature or stress increases, but increase of steady strain rates especially at 1400 °C temperature were much higher than other conditions.

In order to find out the stress and temperature dependence of steady-state creep rates, flexure creep strain–time curves were analyzed in terms of Norton's equation as shown in Eq. (1):

$$\varepsilon_{ss} = A\sigma^n \exp\left(\frac{-Q}{RT}\right) \quad (1)$$

where ε_{ss} is the true steady-state strain rate, A is a constant, σ is the applied stress, T is the absolute temperature, R is the gas constant, n and Q are the stress exponent and the apparent activation energy for creep in the steady-state region, respectively. The tests were performed at constant temperature and different stress, in order to evaluate the stress exponent n, whereas to evaluate the apparent activation energy Q the tests were carried out at constant load and different temperatures. The values of steady-state creep rates of the as-sintered α/β-SiAlON composite ceramic are plotted logarithmically as a function of applied stress for 1400 °C in Fig. 4(a). By the linear fitting of data, the values of the stress exponent n as-sintered α/β-SiAlON composite are determined to be 1.6 ± 0.13 under a stress range of 50–150 MPa. The apparent activation energies of as-sintered α/β-SiAlON composite for creep determined from the steady-state creep rate for 100 MPa are 692 ± 37 kJ/mol in the temperature range of 1300–1400 °C, as shown in Fig. 4(b). The results are in agreement with those reported in the literature for Si_3N_4 and SiAlON ceramics in four point bending creep [7,15–23].

The mechanisms that cause creep and the creep rates of Si_3N_4 and SiAlONs containing intergranular amorphous phase are viscous flow, solution–precipitation, diffusion, grain boundary sliding and cavitation. The active creep mechanism is generally identified by the value of the stress exponent (n). For Si_3N_4 or SiAlON ceramics, stress exponents greater than 3 are found for tensile creep because of the formation of cavities. In compression, the stress exponents are found between 1 and 2 or less than 1 indicative of creep by solution–precipitation. In bending creep, stress exponents are often found between 1 and 3 involving the mechanisms of solution–precipitation, diffusion and grain boundary sliding [13–15]. These variations among the values of stress exponent and activation energy for creep of Si_3N_4 and SiAlON ceramics are due to the processing

Table 1
Steady state creep rates of materials for each creep test conditions.

Material	Tests conditions		Steady state creep rate (ε_{ss}) (s^{-1})
	Temperature (°C)	Stress (MPa)	
α/β-SiAlON	1300	100	9.046×10^{-10} to 1.172×10^{-9}
	1350	100	2.778×10^{-9} to 4.628×10^{-9}
	1400	50–150	7.178×10^{-9} to 6.595×10^{-8}
Si_3N_4	1400	100	1.279×10^{-6}

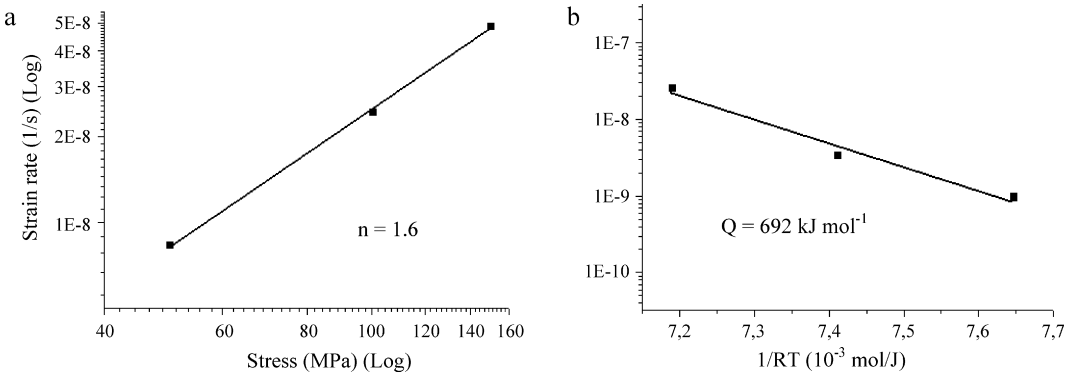

Fig. 4. (a) Stress and (b) temperature dependence of the steady-state creep rate of as-received α/β-SiAlON composite at constant temperature *of* 1400 °C and under constant stress of 100 MPa.

conditions, chemical composition and amount of intergranular phase, the type of creep test (tension or compressive), the temperature and the stress applied during creep tests [23]. The activation energy for creep of Si_3N_4 and SiAlON ceramics is in the range of 550–800 kJ/mol. [7,16–21]. In this study, the stress exponents and activation energies are calculated to be 1.6 ± 0.13 and 692 ± 37 kJ/mol, respectively. Therefore, the creep deformation mechanism for the test conditions used is determined to be grain boundary sliding coupled with diffusion.

In this study, additional flexure creep test of Si_3N_4 material was also conducted to verify the results obtained for SiAlON and compared to well documented Si_3N_4 ceramic in air at temperature of 1400 °C and under 100 MPa stress. The flexure creep strain–time curve obtained in this test under similar conditions to SiAlON is presented in Fig. 5. The Si_3N_4 material showed relatively high strain rate compared to SiAlON, and was fractured after 5 h from start of testing by creep deformation. In contrast, SiAlON deformed around 60% of the total deformation of Si_3N_4 material at the end of 72 h without failure. This result showed that creep resistance of SiAlON ceramic was better than the tested Si_3N_4.

3.3. Phase composition and microstructural characterization of crept materials

XRD analysis of as-sintered bulk sample before and after creep was shown in Fig. 6. The calculations using the relative intensities from XRD analysis revealed that α/β-SiAlON ratio changed due to the oxidation and the transformation from α-SiAlON to β-SiAlON. The α phase content decreased from 20 to 12% and an increase of intergranular amorphous phase crystallization (as melilite) was observed.

Photograph of a typical crept specimen and an as-received specimen is shown in Fig. 7. Visual observation of the crept specimen surfaces revealed the oxidation related effects for the specimen crept at 1400 °C temperature, under 150 MPa stress for more than 100 h with a creep deformation of more than 2% strain. The color of the specimen changed from dark brown to grey after creep test due to oxidation.

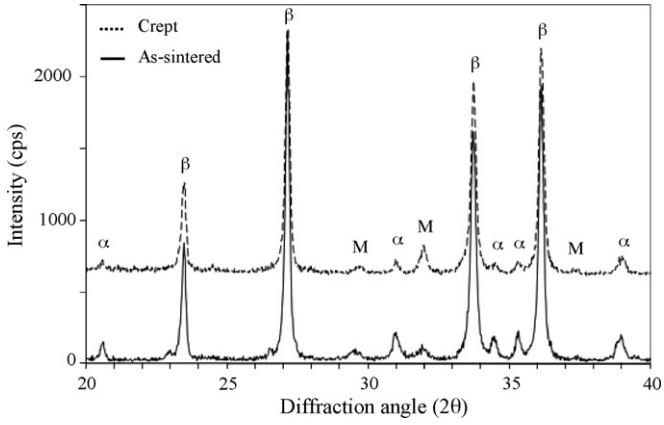

Fig. 6. X-ray diffraction pattern of as-sintered and crept α/β-SiAlON composite (β: beta SiAlON phase, α: alpha SiAlON phase, M: melilite phase ($Ln_2Si_{3-x}Al_xO_{3+x}N_{4-x}$)).

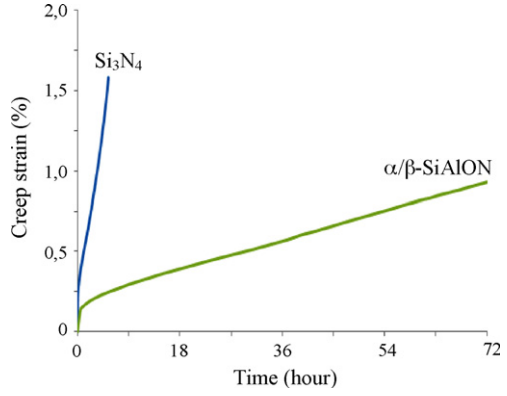

Fig. 5. Creep behavior of as-sintered α/β-SiAlON composite compared to Si_3N_4 at a temperature of 1400 °C under 100 MPa stress.

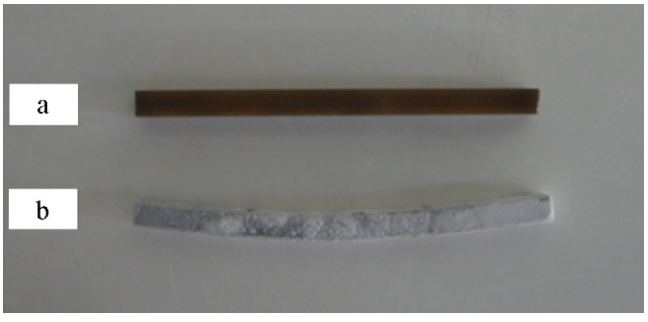

Fig. 7. Visual observation of (a) as-sintered and (b) crept specimens.

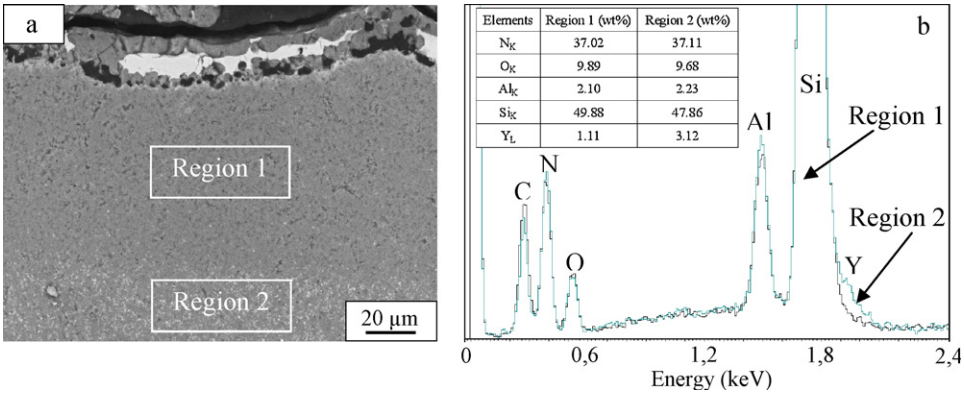

Fig. 8. (a) Back-scattered SEM image of a cross section of the crept specimen and (b) comparative EDX analysis from the depleted zone towards the oxide scale and undepleted zone.

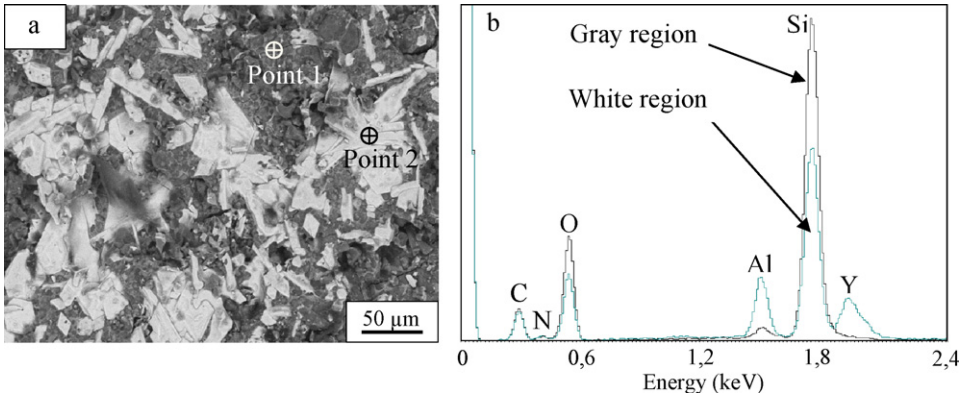

Fig. 9. (a) Back-scattered SEM image of a surface oxide scale and (b) comparative EDX analysis from the white crystals and surrounding regions in the surface oxidation layer.

The characterization of the surface oxidation layer composition was difficult because of the very low intensities in the XRD pattern. Therefore, EDX analysis on SEM were carried out at cross sections and at the oxidized surfaces (Figs. 8 and 9). Fig. 8(a) demonstrates the back-scattered SEM image of a cross section view from the crept sample whereas Fig. 9(a) shows the surface of oxide scale. From the cross sections, it was seen that an oxidation layer and a secondary phase depleted region were formed after creep experiments (Fig. 8(a)). The depletion zone did not contain any of the sintering additives compared to undepleted zone (Fig. 8(b)) whereas the oxidation layer contains oxide phases rich in Y, Al and Si elements along with other sintering additives like Sm and Ca (Fig. 9(b)). These EDX analyse showed that the sintering additives diffused towards the surface of the tested piece and formed oxide phases at the surface.

TEM observations of the crept samples prepared from the tensile stressed oxidation unaffected zone revealed the occurrence of cavities (Fig. 10). All cavities were multigrain-junction

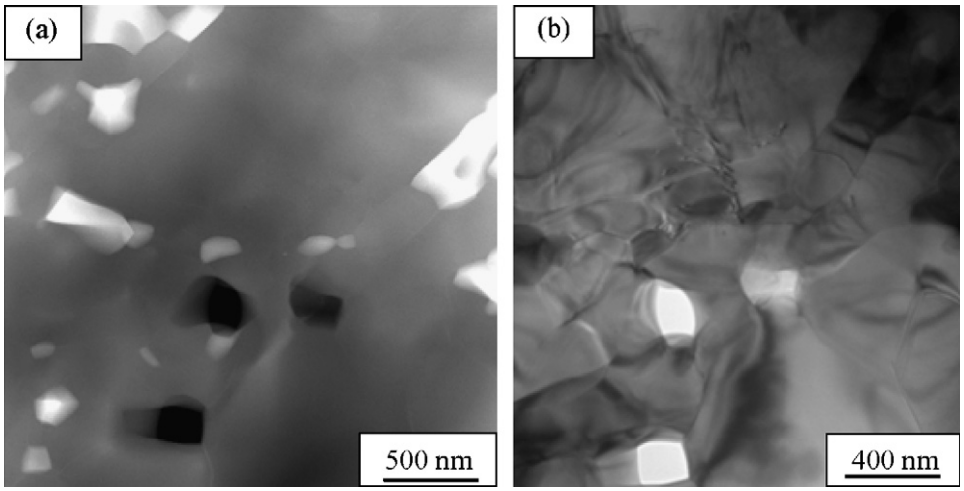

Fig. 10. (a) STEM and (b) TEM images of crept α/β-SiAlON composite showing formation of cavities at multigrain-junctions.

cavities, no other type was found. This observation implies that grain boundary sliding is an important factor for initiation of cavities during creep deformation.

4. Conclusions

The creep behavior of multi cation doped α/β-SiAlON ceramic with melilite as a secondary crystalline phase was assessed by four-point bending creep tests at temperatures from 1300 °C to 1400 °C under stresses from 50 to 150 MPa in air. The stress exponent and creep activation energy were determined to be 1.6 ± 0.13 and 692 ± 37 kJ/mol^{-1}, respectively and grain boundary sliding coupled with diffusion was identified as the rate-controlling creep mechanism for the α/β-SiAlON composite. As the creep mechanism was determined to be grain boundary sliding coupled with diffusion, the reduction of intergranular amorphous phase by the formation of melilite phase, reduce the creep deformation and this result in the improved creep resistance of these ceramics. Therefore, the SiAlON system presents numerous opportunities for further development. The presence of a number of crystalline secondary phases forming in the system can be utilized for the improvement of high temperature properties. However, more understanding is needed on the effect of dopant type and composition in order to obtain better crystallization and improved grain boundary chemistry for creep behavior of these ceramics.

Acknowledgements

We would like to thank MDA Advanced Ceramic Technology A.Ş. for supplying of α/β-SiAlON composites, Mr. Hilmi Yurdakul and Miss Sinem Kayhan for their help on microscopy investigations and Prof. Dr. Servet Turan for useful discussions.

References

[1] S. Hampshire, Silicon nitride ceramics, Mater. Sci. Forum 606 (2009) 27–41.
[2] F.L. Riley, Silicon nitride and related materials, J. Am. Ceram. Soc. 83 (2000) 245–265.
[3] S. Hampshire, H.K. Park, D.P. Thompson, K.H. Jack, α′-SiAlON ceramics, Nature 274 (5674) (1978) 880–882.
[4] H. Mandal, New developments in α-SiAlON ceramics, J. Eur. Ceram. Soc. 19 (13-14) (1999) 2349–2357.
[5] H. Klemm, M. Herrmann, T. Reich, C. Schubert, High-temperature properties of mixed α/β-SiAlON materials, J. Am. Ceram. Soc. 81 (5) (1998) 1141–1148.
[6] A.A. Wereszczak, T.P. Kirkland, M.K. Ferber, T.R. Watkins, R.L. Yeckley, The effects of residual phase on the creep performance at 1370 °C of yttria-doped HIPed silicon nitride, J. Mater. Sci. 33 (1998) 2053–2060.
[7] M.K. Cinibulk, G. Thomas, S.M. Johnson, Strength and creep behavior of rare-earth disilicate-silicon nitride ceramics, J. Am. Ceram. Soc. 75 (8) (1992) 2050–2055.
[8] N.C. Acikbas, A. Kara, S. Turan, F. Kara, H. Mandal, B. Bitterlich, Influence of type of cations on intergranular phase crystallisation of SiAlON ceramics, Mater. Sci. Forum 554 (2007) 119–122.
[9] C.P. Gazzara, D.R. Messier, Determination of phase content of Si_3N_4 by X-ray diffraction analysis, Am. Ceram. Soc. Bull. 56 (9) (1977) 777–780.
[10] G. Ziegler, Thermo-mechanical properties of silicon nitride and their dependence on microstructure, Mater. Sci. Forum 47 (1989) 162–203.
[11] G.E. Gazza, Examining Si_3N_4 base materials with various rare earth additions, U.S. army materials technology laboratory MTL TR 91-45 AD-A243 66S (1991).
[12] A.A. Wereszczak, M.K. Ferber, T.P. Kirkland, A.S. Barnes, E.L. Frome, M.N. Menon, Asymmetric tensile and compressive creep deformation of hot-isostatically-pressed Y_2O_3-doped-Si_3N_4, J. Eur. Ceram. Soc. 19 (1999) 227–237.
[13] S.M. Wiederhorn, B.J. Hockey, J.D. French, Mechanisms of deformation of silicon nitride and silicon carbide at high temperatures, J. Eur. Ceram. Soc. 19 (1999) 2273–2284.
[14] J.J. Melendez Martinez, A. Dominguez-Rodriguez, Creep of silicon nitride, Prog. Mater. Sci. 49 (2004) 19–107.
[15] M.H. Bocanegra-Bernala, B. Matovic, Mechanical properties of silicon nitride based ceramics and its use in structural applications at high temperatures, Mater. Sci. Eng. A 527 (2010) 1314–1338.
[16] K.M. Fox, J.R. Hellmann, Microstructure and creep behavior of silicon nitride and SiAlONs, Int. J. Appl. Ceram. Technol. 5 (2008) 138–154.
[17] M.T. Lin, J.L. Shi, L. Wang, D.Y. Jiang, M.L. Ruan, T.R. Lai, Microstructure and creep behavior of an Y-α-β SiAlON composite, J. Eur. Ceram. Soc. 21 (2001) 833–840.
[18] M.T. Lin, L. Wang, D.Y. Jiang, G.Q. Zhu, J.L. Shi, High temperature bending creep of a Sm-α-β SiAlON composite, J. Mater. Sci. 37 (2002) 655–662.
[19] J.A. Todd, Z.-Y. Xu, The high temperature creep deformation of Si_3N_4–$6Y_2O_3$–$2Al_2O_3$, J. Mater. Sci. 24 (1989) 4443–4452.
[20] Y.R. Xu, X.R. Fu, D.S. Yan, Creep behavior of hot-pressed silicon nitride ceramics with rare-earth oxides and alumina additives, Physica B 150 (1988) 276–282.
[21] B.S.B. Karunaratne, M.H. Lewis, High-temperature fracture and diffusional deformation mechanisms in Si–Al–O–N ceramics, J. Mater. Sci. 15 (1980) 449–462.
[22] M.K. Ferber, M.G. Jenkins, V.J. Tennery, Comparison of tension, compression and flexural creep for alumina and silicon nitride, Ceram. Eng. Sci. Proc. 11 (7) (1990) 1028–1045.
[23] W.R. Cannon, T.G. Langdon, Review, creep of ceramics. Part 1. Mechanical characteristics, J. Mater. Sci. 18 (1983) 1–50.